GEOLOGY | THE GEOLOGICAL SOCIETY OF AMERICA®

https://doi.org/10.1130/G47079.1

Manuscript received 7 October 2019
Revised manuscript received 22 January 2020
Manuscript accepted 31 March 2020

Published online 18 May 2020

A sub-centennial-scale optically stimulated luminescence chronostratigraphy and late Holocene flood history from a temperate river confluence

Ben Pears[1], Antony G. Brown[1,2], Phillip S. Toms[3], Jamie Wood[3], David Sanderson[4] and Richard Jones[5]

[1]Palaeoenvironmental Laboratory, Department of Geography and Environmental Science, University of Southampton, Highfield Campus, University Road, SO17 1BJ Southampton, UK

[2]Natural Sciences, Tromsø University Museum, Arctic University of Norway, 9013 Tromsø, Norway

[3]Luminescence Dating Laboratory, School of Natural and Social Sciences, University of Gloucestershire, Swindon Road, GL50 4HZ Cheltenham, UK

[4]Scottish Universities Environmental Research Centre, Rankine Avenue, Scottish Enterprise Technology Park, G75 0QF East Kilbride, UK

[5]Centre for English Local History, University of Leicester, Salisbury Road, LE1 7RH Leicester, UK

ABSTRACT

River confluences can be metastable and contain valuable geological records of catchment response to decadal- to millennial-scale environmental change. However, in alluvial reaches, flood stratigraphies are particularly hard to date using ^{14}C. In this paper, we use a novel combination of optically stimulated luminescence and multiproxy sedimentological analyses to provide a flood record for the confluence of the Rivers Severn and Teme (United Kingdom) over the past two millennia, which we compare with independent European climate records. The results show that by ca. 2000 yr B.P., the Severn-Teme confluence had stabilized and overbank alluviation had commenced. Initially, this occurred from moderately high flood magnitudes between ca. 2000 and 1800 yr B.P. (50 BCE–150 CE), but was followed from 1800 to 1600 yr B.P. (150–350 CE) by fine alluvial deposition and decreased flood intensity. From 1600 to 1400 yr B.P. (350–550 CE), the accumulation rate increased, with evidence of large flood events associated with the climatic deterioration of the Dark Age Cold Period. Following a period of reduced flood activity after ca. 1400 yr B.P. (ca. 550 CE), larger flood events and increase in accumulation rate once again became more prevalent from ca. 850 yr B.P. (ca. 1100 CE), coincident with the start of the Medieval Climate Anomaly, a period associated with warmer, wetter conditions and increased land-use intensity. This state persisted until ca. 450 yr B.P. (ca. 1500 CE), after which increased flood magnitudes can be associated with climatic variations during the Little Ice Age. We demonstrate that from the combination of high-resolution dating techniques and multiple analytical parameters, distinctive phases of relative flood magnitude versus flood duration can be determined to a detailed chronological precision beyond that possible from ^{14}C dating. This permits the identification of the regional factors behind floodplain sedimentation, which we correlate with the intensification of land-use and climatic drivers over the last two millennia.

INTRODUCTION

River floodplains contain archives of changing climatic and catchment conditions through their extensive sedimentary records. In particular, confluence zones act as nodal points for flooding, because floodplains are generally at their widest and integrate flood peaks from several catchments. Confluence migration can happen through channel-belt movements as well as from meander-migration and/or through meander cutoffs (Best and Lane, 2004; Camporeale et al., 2007; Brown et al., 2013; Dixon et al., 2018). Additionally, oscillatory channel behavior can also occur, stimulated by large floods (Brown et al., 2013). However, some confluences can be surprisingly stable, becoming fixed or pinned when confined by tall banks created by high rates of levee and/or overbank deposition (Dixon et al., 2018). It is these large volumes of overbank sediment stored in confluence zones that act as archives of flooding and past catchment conditions.

In upland reaches, ^{14}C probability density functions can yield depositional histories from channel and flood deposits (Macklin et al., 2010), but many ^{14}C-derived chronostratigraphies terminate before 1000 yr B.P. as a result of sediment reworking and organic translocation, leading to problems with the calibration of dates. Additionally, in clastic-dominated alluvial sequences, suitable organic material is only occasionally encountered, and, where it is, its reliability for dating is also questionable. These factors have made it difficult to relate the sedimentary record to documentary or instrumental flood histories, which in Europe rarely go back further than 100–250 yr (Macdonald and Sangster, 2017; Longfield et al., 2018). In this paper, we show how the confluence of the Rivers Severn and Teme (United Kingdom) has evolved over the past two millennia. We reconstruct overbank sedimentation and a detailed flood history using extensive optically stimulated luminescence (OSL) dating, alongside detailed stratigraphic and sedimentological analyses.

CONFLUENCE METASTABILITY

The Severn-Teme confluence (centered on 52.166947°N, 2.2303104°W) has >5 m of overbank sediments deposited unconformably on channel gravels. Both the Severn (4325 km^2) and Teme (1648 km^2) catchments drain the Cambrian Mountains, receiving mixed-intensity precipitation from west-to-east cyclonic activity and depression systems. The 3.5 km^2 confluence zone is bounded by Pleistocene gravel terrace deposits with alluvium deriving from the

CITATION: Pears, B., et al., 2020, A sub-centennial-scale optically stimulated luminescence chronostratigraphy and late Holocene flood history from a temperate river confluence: Geology, v. 48, p. 819–825, https://doi.org/10.1130/G47079.1

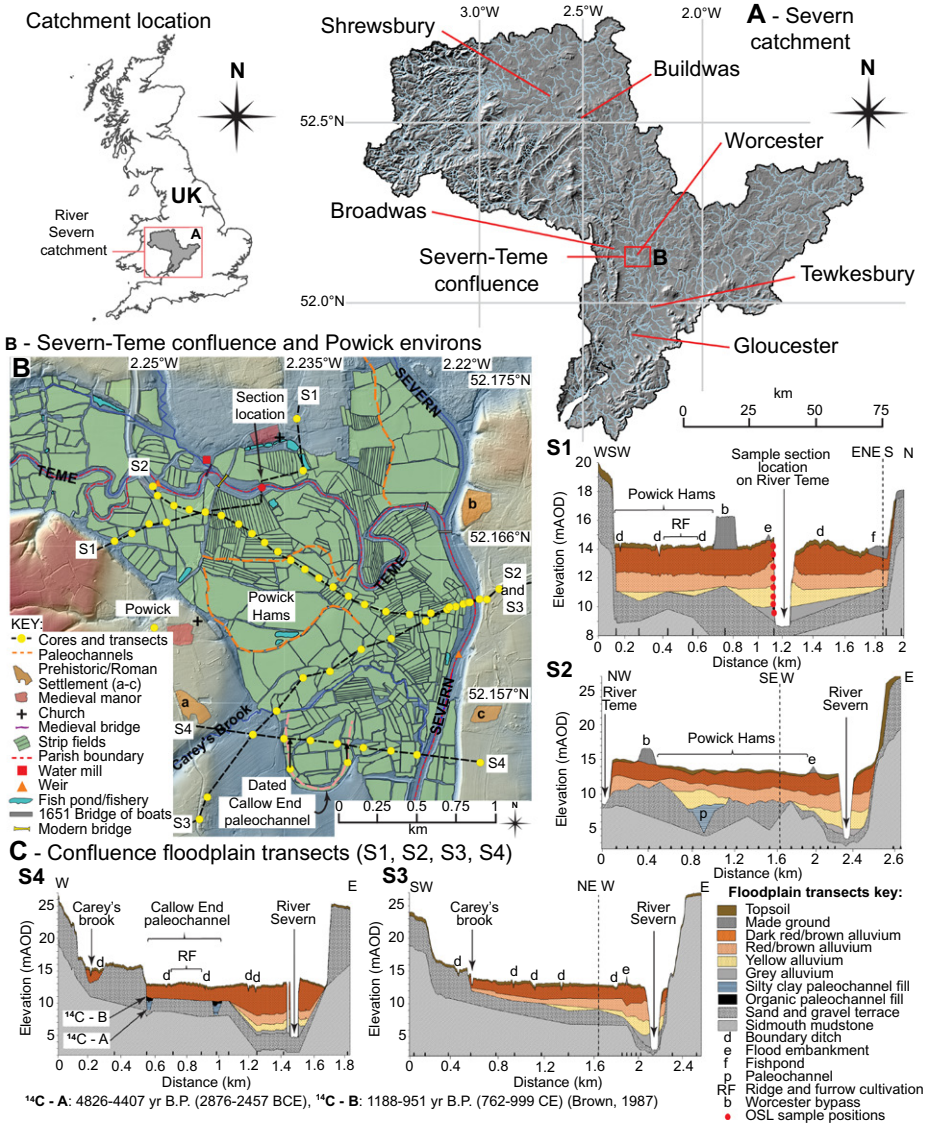

Figure 1. (A) River Severn catchment (UK), major settlements, and other sample locations (see Fig. 4). Base map is 50-m-resolution lidar digital terrain model (DTM) (UK Ordnance Survey, 2016). (B) River Severn–River Teme confluence on 1-m-resolution lidar DTM base map SO85SW, SO85SE (UK Environment Agency, 2016), showing core locations (British Geological Survey, 2017), river section location (red dot), and paleochannels (dated, pink; undated, orange). Historic land use is plotted from 1 m lidar, Coventry map (ca.1648 CE, Herefordshire and Worcestershire Record Office, BA940, folio 970.7.73), UK Ordnance Survey (UK Ordnance Survey, 1886), and Worcestershire Historic Environment Record (http://www.worcestershire.gov.uk/archaeology). (C) Reconstructed and modeled floodplain cross sections (S1–S4) with surface topography extracted from 1 m lidar DTM and shown as elevation in meters above Ordnance Datum (mAOD) against distance (km) across floodplain. Sedimentological data were extracted from core data (Brown, 1987; British Geological Survey, 2017) and, historic features were marked from a county historic environment record (Worcestershire Historic Environment Record).

basal Triassic mudstone, siltstone, and sandstone lithologies (Fig. 1). Deep clastic alluvial deposits of the Severn-Teme confluence were first identified more than 30 years ago (Brown, 1985) but were undatable due to a lack of suitable organic material for ^{14}C dating. However, a chronostratigraphy of channel change in the reach was established by dating paleochannel sediments within the confluence zone (Brown, 1987). The dating of a large meander of the Teme, which must once have been close to the junction with the Severn, shows that it was abandoned by progressive avulsion to the north between 4826 and 4407 yr B.P. (2876–2457 BCE). The remodeling of borehole data across the confluence shows an undated paleochannel below the overbank units, which most likely demonstrates an intermediate position prior to the creation of the large gooseneck-type meander characteristic of the present Teme channel. Alongside the physical evidence, historical data also confirm channel stability. The earliest detailed cartographic evidence shows that the Teme had adopted its current course by 1648 CE, and the permanency of parish boundaries, which continue to follow the present river course, as well as the location of medieval mills, leats (artificial watercourses or aqueducts supplying water to watermills), and weirs (low head dams) all indicate channel stability from as early as 1188–951 yr B.P. (762–999 CE) (Fig. 1). The extensive depths of sandy silts blanketing the paleochannels can be traced across the confluence and further afield, including the River Avon catchment to the east. This unit was originally designated the "buff red silty clay" (Shotton 1978) and shown to postdate ca. 3600 yr B.P. (ca. 1650 BCE) in all locations.

The stratigraphy of the sampled Powick section (52.169259°N, 2.2376946°W) (Fig. 2) consists of a lower unit of 0.6 m of yellowish-gray medium to fine sandy silt (unit A), overlain by 2.3 m of dark-yellow to reddish-brown fine silt (unit B), covered by 1.1 m of reddish-brown medium sandy silt (unit C), capped by 0.8 m of dark reddish-brown coarse sandy silt and a 0.4 m soil horizon (unit D). Faint, but clear, sand-silt laminations were identified and recorded throughout. These could be traced the entire length of the section (150 m) and correspond to a sequence previously recorded ~500 m upstream (Brown, 1985). This confirms that the sequence dated and analyzed here is representative of the confluence as a whole, and that the rate of overbank deposition was high enough to outpace rare bioturbation by earthworms.

SAMPLING AND ANALYSIS

Eight OSL dates and *in situ* dosimetry were taken at 0.4–0.8 m intervals up-sequence (see the Supplemental Material[1], Data Set S3). Sediment u-channels (method to obtain longitudinal *in-situ* sediment samples from cylindrical cores and sections) ranging from 0.3 to 0.4 m in length were extracted for detailed sedimentary analysis (loss on ignition [LOI], magnetic susceptibility

[1]Supplemental Material. Supplemental Sections S1–S16; Figures S1 (sediment accumulation rate modeled by OxCal and Bacon) and S2 (relative moisture values between OSL and LOI analytical methods); Table S1 (OSL procedure from the Rivers Severn-Teme confluence at Powick, UK); and Data Sets S1 (raw data for the modeled calendric dates, sediment accumulation rate, and sedimentological analyses), S2 (raw and log normalized data for ITRAX XRF analysis and key elements Zr, Rb, Fe, Mn, and heavy metals illustrated in Fig. 2), S3 (individual raw data sets for each 5 cm pOSL run alongside a background sediment sample and a summary sheet of all data and replicates), S4 (raw data, log normalized data, and statistical analysis used in the agglomerative hierarchical cluster analysis illustrated in Fig. 2), S5 (calculated log data of sedimentary analyses by 50 yr period and the statistical analysis used in the principal component analysis illustrated in Fig. 3), and S6 (20 yr grouping for the sediment deposition models for the Severn-Teme confluence at Powick, Broadwas, and Buildwas and climatic datasets illustrated in Fig. 4). Please visit https://doi.org/10.1130/GEOL.26213S.12250157 to access the supplemental material, and contact editing@geosociety.org with any questions.

[MS], and particle size), alongside multi-elemental analysis using an ITRAX X-ray fluorescence (XRF) scanner (Supplemental Material Sections S5–S9; Data Sets S1 and S2). Additional bulk samples were taken every 5 cm, from 10 cm into the cleaned river section to shield them from light, and subjected to luminescence profiling using a portable reader (portable optically stimulated luminescence, pOSL) (Section S10; Data Set S3). Age-depth Bayesian modeling of the dated alluvial sequence was initially conducted using the OSL settings provided by OxCal software version 4.3 with the IntCal13 calibration curve (Bronk Ramsey 2008, 2009) and then using Bacon software version 2.2 (Blaauw and Christen 2011) to provide a cross-reference of chronological quality as well as improved calendric date output (2σ [95.4%] and 1σ [68.2%] precision) (Fig. 2; Sections S3 and S4; Table S1) and sediment accumulation rate (~1.8–3.2 mm/yr). Statistical analysis of data was conducted to clarify depositional processes (Sections S11 and S12; Data Sets S4 and S5), and sediment index models created to compare against climatic data (Section S14; Data Set S6).

SEDIMENTARY PARAMETERS

The sequence is entirely clastic except for the top 0.4 m associated with contemporary soil formation and increased organic matter (Fig. 2). High-temperature LOI shows several peaks within periods of finer sedimentation reflecting carbonate, but also small increases in mixed layer, clays that are present in the basal Mercia Mudstone geology. MS peaks are most likely due to increases in Fe minerals associated with ironstones, heavy minerals, and coatings of quartz grains typical of the aeolian-derived Triassic sands in the Teme catchment. Particle size fractions are taken to reflect flow velocities delivered to the floodplain and would reflect flood velocity if the location of the channel were constant relative to the site. The power function combines the coarse sediment fraction (D_{90}, coarsest grain size percentile), a proxy for flow velocity, with organic matter percentage (an inverse function of sedimentation rate). Measurements of mineralogy were undertaken using the ITRAX XRF Scanner (Croudace et al., 2006) to calculate log Zr:Rb ratios. This provides a measure of the weathered nature of the sediment and the relative contribution of detrital grains versus clay minerals.

In order to refine the depositional history and determine flood events, pOSL analysis was conducted (Sanderson and Murphy, 2010). The technique has proven success in fluvial contexts (Muñoz-Salinas et al., 2010) (Section S10), and demonstrates that sudden changes and particularly peaks in accumulated pulsed infrared stimulated luminescence (pIRSL) dose that diverge from general trends identify sources of sediment that are relatively unbleached and derive from eroded bank sediment and mobilized during high-energy flow events. Periods of constant flood rate with equally sized events would produce a uniform pOSL curve.

DISCUSSION

From the age-depth model and sedimentary properties, it is possible to propose a flood history for the midpoint of the Severn catchment over the past 2000 yr (Fig. 2). From 2000 to 1800 yr B.P. (50 BCE–150 CE), medium-silt alluvium with elevated proportions of sand and pOSL are present and possibly reflect increased soil erosion from the Late Iron Age and Romano-British cultivation, similar to other major United Kingdom lowland floodplains (Robinson and Lambrick, 1984; Brown, 2009). Between 1800 and 1600 yr B.P. (150–350 CE), there is a reduction in sand and increase in carbonate and fine particulates, indicating a reduction in fluvial depositional conditions. After 1600 yr B.P. and continuing until 1400 yr B.P. (550 CE), fine alluvial sedimentation continued, but an increase in accumulation rate and clear peaks in MS demonstrate large, lower-energy flood events at the start of the Dark Age Cold Period in response to climatic downturn (Lamb 1972). The development of extensive floodplain meadowlands across many river systems at this time may have, in part, been as a result of suitable "well-watered" conditions (Williamson 2013, 204). There followed from 1400 to 1100 yr B.P. (550–850 CE) a fall in accumulation rate and lower-energy alluviation, with increases in carbonate and pOSL after 1250 yr B.P. (700 CE).

From 1100 to 600 yr B.P. (850–1350 CE), the sedimentological evidence suggests higher fluvial activity with an increase in high-magnitude events. The accumulation rate increases markedly alongside more numerous peaks in MS, higher sand content, and increases in pOSL and elemental indicators. This clear change corresponds with the change to warmer, wetter conditions typical of the Medieval Climate Anomaly alongside increased land-use intensity on the floodplain. At this time, arable cultivation covered 30%–50% of the total land area in those English counties within the Severn-Teme catchment (Broadberry et al., 2015; Rippon et al., 2015) and beyond (Hey 2004), corresponding to peak medieval population levels in midland England of >10 persons/km^2 (Goldewijk et al., 2010).

From 600 to 400 yr B.P. (1350–1550 CE), river conditions appear to have calmed, and a sharp decrease in accumulation rate alongside increase in carbonate and reduction in other proxies suggest fewer high-energy depositional events. After 400 yr B.P. (1550 CE) and continuing through to the present, there is another rise in accumulation rate alongside a significant increase in grain size to coarse silt, considerably higher sand content, and major increases in pOSL and elemental indicators. Together these demonstrate intensive phases of deposition in the Severn-Teme confluence, particularly 400–350 yr B.P. (1550–1600 CE), 250–200 yr B.P. (1700–1750 CE), and ca. 100 yr B.P. (1850 CE), and appear conterminous with the period of maximum recorded historical flood events (Marsh et al., 2016; Macdonald and Sangster, 2017) and the abandonment of the open-field system. The data support the identification of periods of shorter-duration but higher-magnitude flood-dominated regimes caused by increased snowmelt and storminess (Rumsby and Macklin, 1996; Macklin et al., 2012).

Statistically there are clear relationships between the key analytical results (Fig. 3). There is a positive correlation between grain size, sand content, and Zr:Rb associated with a higher coarse component within the alluvium. A positive trend is also present for pIRSL and pOSL, although there is less-clear correlation between the overall particle size and pOSL, possibly as a result of variations in sediment provenance. Clear negative correlations are present between (1) the aforementioned classes, and (2) carbonate and, to a lesser extent, magnetic susceptibility.

The stratigraphic variation at the Severn-Teme confluence can now be compared to that of other recently established deep alluvial sequences along the Rivers Teme and Severn (Pears et al., 2020), providing further evidence for flood regimes in other parts of their catchments, as well as to European-scale climatic models to assess potential drivers (Fig. 4). All three fluvial sequences demonstrate predominantly fine-grained deposition to 1450 yr B.P. (350 CE) during the Roman Warm Period associated with warmer, drier conditions across the United Kingdom, Ireland, and Europe (Charman et al., 2006; Swindles et al., 2013; Wilson et al., 2013; Büntgen et al., 2011; Fig. 4A). In contrast, from 1500 to 1000 yr B.P. (400–1100 CE), the sedimentary models from the upstream profiles at Broadwas and Buildwas demonstrate much-coarser sediment deposition than at the Severn-Teme confluence, suggesting that the variable climatic conditions of the Dark Age Cold Period and Medieval Climate Anomaly had more localized effects upon the fluvial activity in the upper reaches of these river systems (Fig. 4B). The onset of significantly coarser sedimentation in the Severn-Teme confluence from 900 yr B.P. (1000 CE), which accelerated after 400 yr B.P. (1550 CE), is mirrored in the other sequences albeit with longer phases of finer sediment deposition, and can be associated with climatic variability during the Little Ice Age (Wanner et al., 2008; Phipps et al., 2013), leading to prolonged phases of wetter conditions across the United Kingdom and Ireland (Charman et al., 2006; Swindles et al., 2013; Wilson et al. 2013) and cooler European climates (Esper et al., 2014; Fig. 4C), as well as continued intensification of

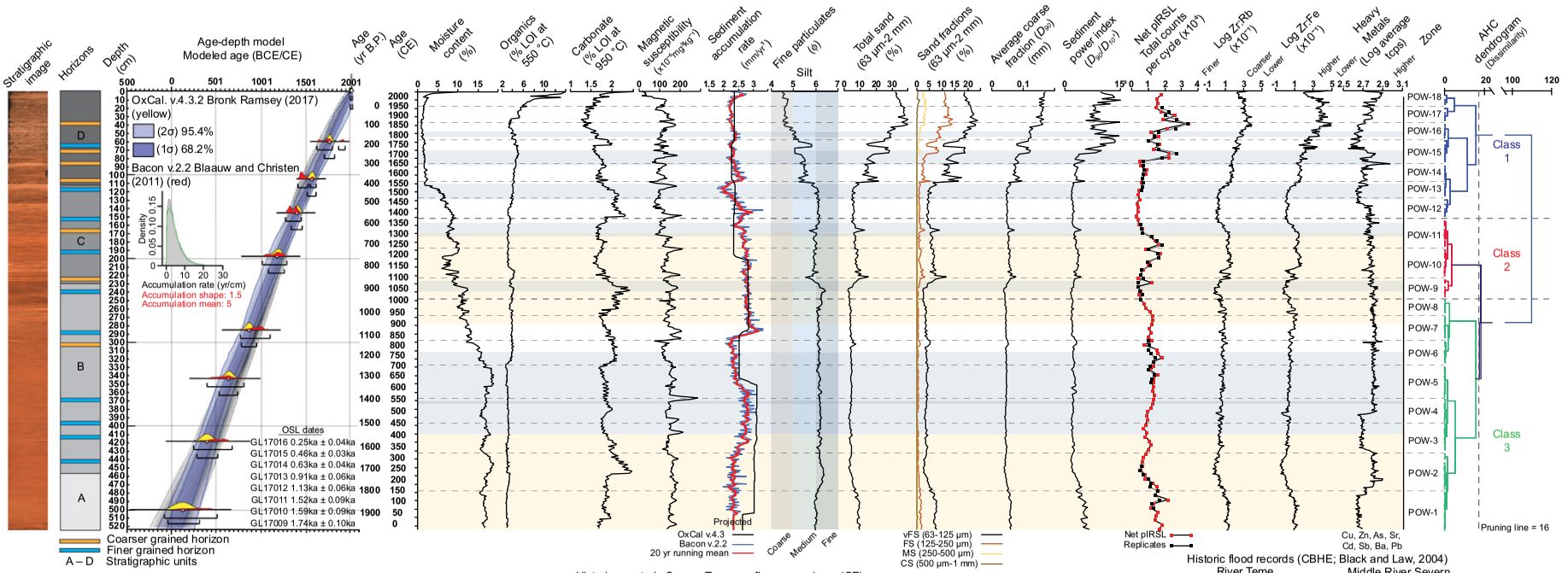

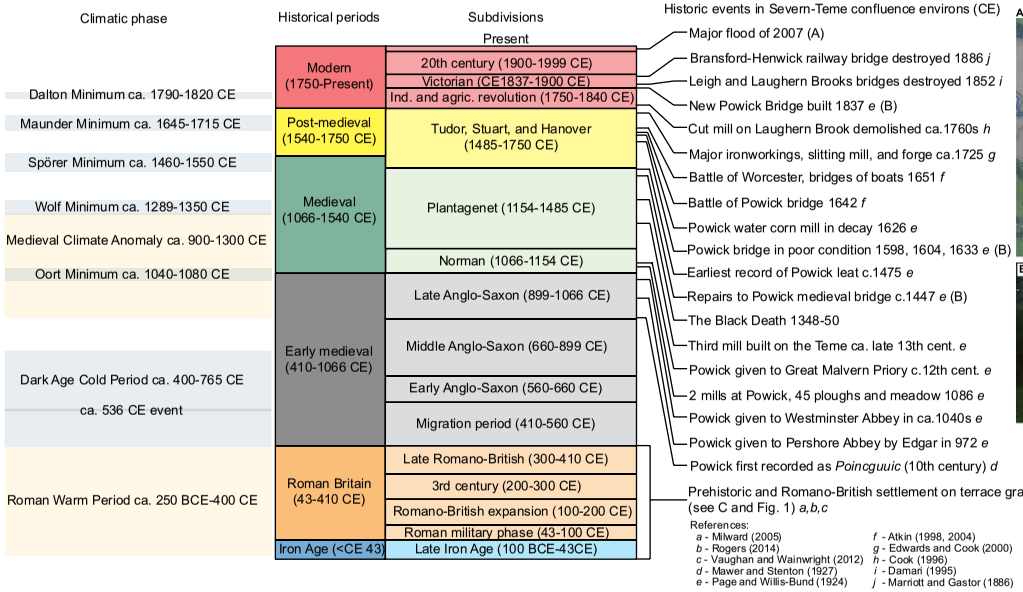

Historic events in Severn-Teme confluence environs (CE)

- Major flood of 2007 (A)
- Bransford-Henwick railway bridge destroyed 1886 *j*
- Leigh and Laughern Brooks bridges destroyed 1852 *i*
- New Powick Bridge built 1837 *e* (B)
- Cut mill on Laughern Brook demolished ca.1760s *h*
- Major ironworkings, slitting mill, and forge ca.1725 *g*
- Battle of Worcester, bridges of boats 1651 *f*
- Battle of Powick bridge 1642 *f*
- Powick water corn mill in decay 1626 *e*
- Powick bridge in poor condition 1598, 1604, 1633 *e* (B)
- Earliest record of Powick leat c.1475 *e*
- Repairs to Powick medieval bridge c.1447 *e* (B)
- The Black Death 1348-50
- Third mill built on the Teme ca. late 13th cent. *e*
- Powick given to Great Malvern Priory c.12th cent. *e*
- 2 mills at Powick, 45 ploughs and meadow 1086 *e*
- Powick given to Westminster Abbey in ca.1040s *e*
- Powick given to Pershore Abbey by Edgar in 972 *e*
- Powick first recorded as *Poincguuic* (10th century) *d*

Prehistoric and Romano-British settlement on terrace gravels (see C and Fig. 1) *a,b,c*

References:
a - Milward (2005)
b - Rogers (2014)
c - Vaughan and Wainwright (2012)
d - Mawer and Stenton (1927)
e - Page and Willis-Bund (1924)
f - Atkin (1998, 2004)
g - Edwards and Cook (2000)
h - Cook (1996)
i - Damari (1995)
j - Marriott and Gastor (1886)

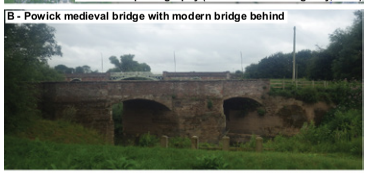

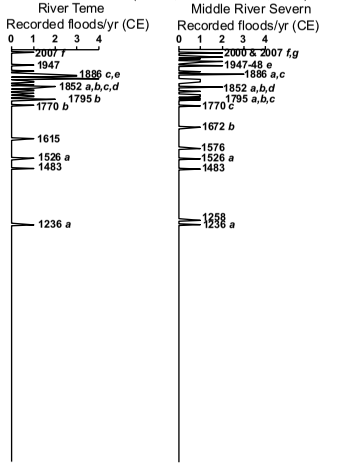

References:
a - Damari (1995)
b - Southall (1895)
c - Marriott and Gaster (1886)
d - Annual Register of 1852, (1853)
e - Symons (1887)
f - Marsh and Hannaford (2007)

References:
a - Damari (1995)
b - Marriott and Gaster (1886)
c - Southall (1895)
d - Annual Register of 1852, (1853)
e - NERC (1975)
f - Marsh and Dale (2002)
g - Marsh and Hannaford (2007)

Figure 2. Stratigraphic image with interpreted horizons and stratigraphic units; Age-depth model using OxCal. v.4.3.2 (yellow) (Bronk Ramsey, 2017), and Bacon v.2.2 (red) (Blaauw and Christen, 2011) of each optically stimulated luminescence (OSL) date with entire date range (black horizontal line), and calculated statistical ranges at 1σ (68.2%) and 2σ (95.4%) variation (black brackets). Purple and grey shading demonstrates statistical range across sequence at 1σ and 2σ. The density-accumulation rate graph of the Bacon model demonstrates an overall uniform rate of deposition, with a mean accumulation of 5 yr/cm. However, more detailed variation in sediment accumulation rate is also presented. Both the OxCal and Bacon methods show a similar overall pattern but more discrete variation is illustrated in the Bacon model. Also shown are loss on ignition (LOI) for moisture (at 105 °C for 12 h), organics (at 550 °C for 2 h) and, carbonate content (at 950 °C for 4 h); magnetic susceptibility; fine and coarse sediment textural characteristics, defined by particle size analysis (vFS—very fine sand; FS—fine sand; MS—medium sand; CS—coarse sand; D_{90}—coarsest sediment fraction); sediment power index, calculated as coarse fraction divided by the cubed proportion of fine fraction (D_{90}/D_{10}^3); sediment texture also defined by portable optically stimulated luminescence (pOSL) as shown by net pulsed infra-red stimulated luminescence (pIRSL); ITRAX XRF log Zr:Rb (finer to coarser); ;og Zr:Fe (lower to higher flood event indicator), and ;og average total counts per second (tcps) heavy metals (lower to higher) (Cu, Zn, As, Sr, Cd, Sb, Ba, Pb). The Agglomerative Hierarchical Analysis (AHC) demonstrates the statistical classification of sediment types in the sequence and their dissimilarity from each other. At Powick, UK, three clear classes have been determined (Class 3—ca. 50 BCE to 1000 CE; Class 2—ca. 1000 to 1375 CE; Class 1—ca. 1375 to present, and specifically after 1550 CE). This reflects increasing up-sequence variation in texture and grain-size from increasingly higher energy flood deposition. Vertical dashed line represents the calculated pruning line from which the cluster variation has been computed. Alongside the main classes, refined statistical zones (POW-1 to POW-18) are marked, reflecting intra-class cluster variation across the sequence. Bottom row of the figure shows mainly qualitative data sets including climatic phase (colder—light blue; warmer—yellow) with the name and period of duration. UK historical periods and subdivisions (Industrial and agricultural revolution [Ind. and agric. Revolution]); historic events within the Severn-Teme confluence; orthophotography of extent of the 2007 flood, recently matched or exceeded by 2020 flood; images of Powick medieval and modern bridges, and an example of prehistoric and Romano-British settlement evidence on the floodplain edge (location shown in Fig. 1). Final section shows the number of recorded floods per year from the Teme and Severn, with exceptional events illustrated by dates. Both models show a clear increase in larger floods after ca. 1500CE which corresponds with the period of greatest fluvial activity in the sediment model. See the Supplemental Material (see footnote 1) for methods, data, and references.

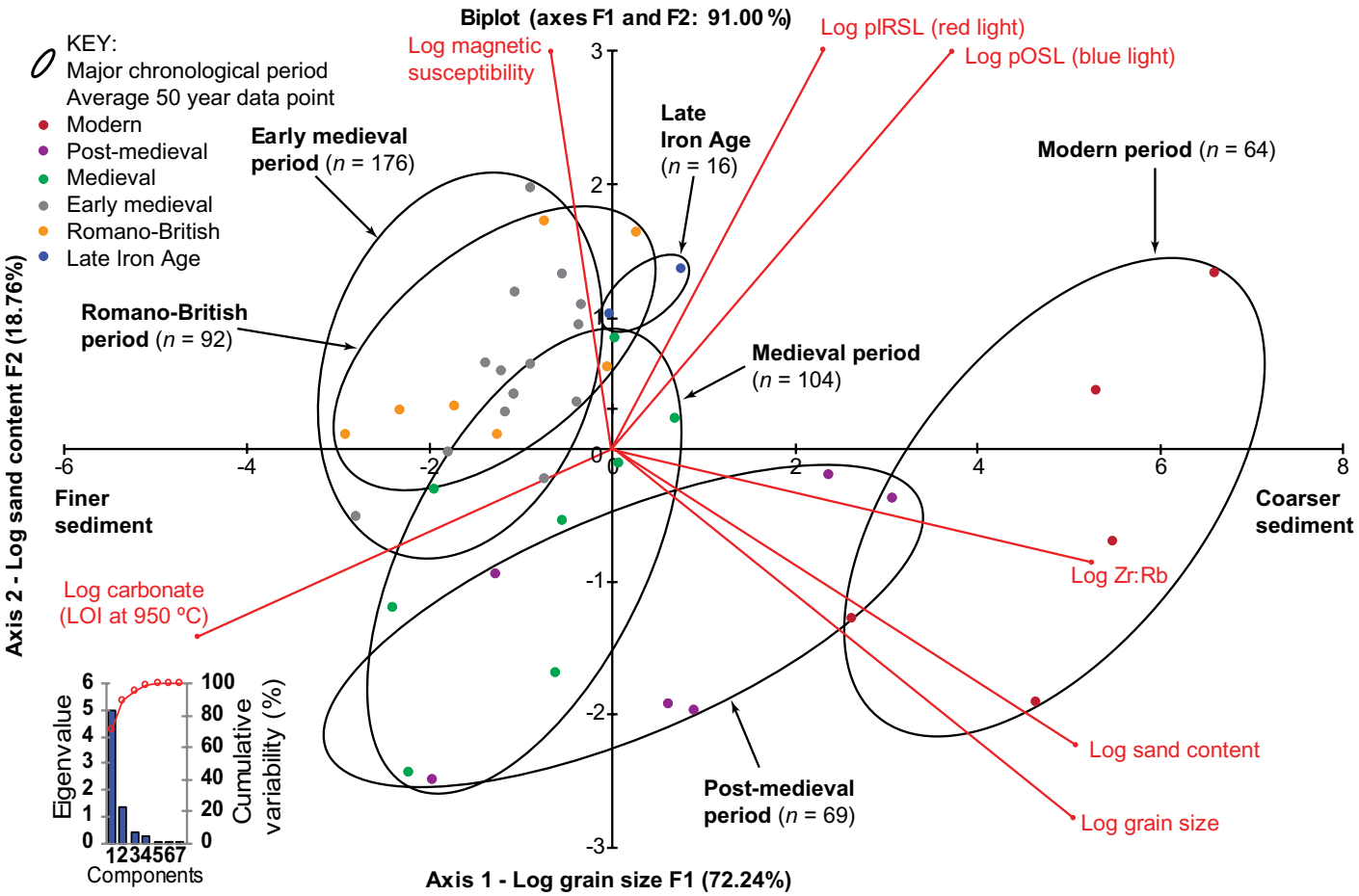

Figure 3. Principal component analysis (PCA) using XLSTAT software (version 2019.2.3, https://www.xlstat.com/en/) conducted across seven key proxy texture variables (red lines): log pulsed infra-red stimulated luminescence (pIRSL, red light); log pulsed optically stimulated luminescence (pOSL, blue light); log Zr:Rb; log sand; ;og grain size; log magnetic susceptibility; and log carbonate derived by loss on ignition (LOI) at 950 °C. Stratigraphic observations (n = 521) were clustered across 50 yr time spans from 20 BCE to present and placed into the biplot based upon the Eigenvalues of the two major components lLog grain size versus log % sand), and the results classed into six Late Holocene time periods (black ellipses). The biplot percentage (91%) represents the proportion of the total data used in the model and the percentages of each axis (log grain size 72.24% and log sand content 18.76%) show the proportion across the two components.

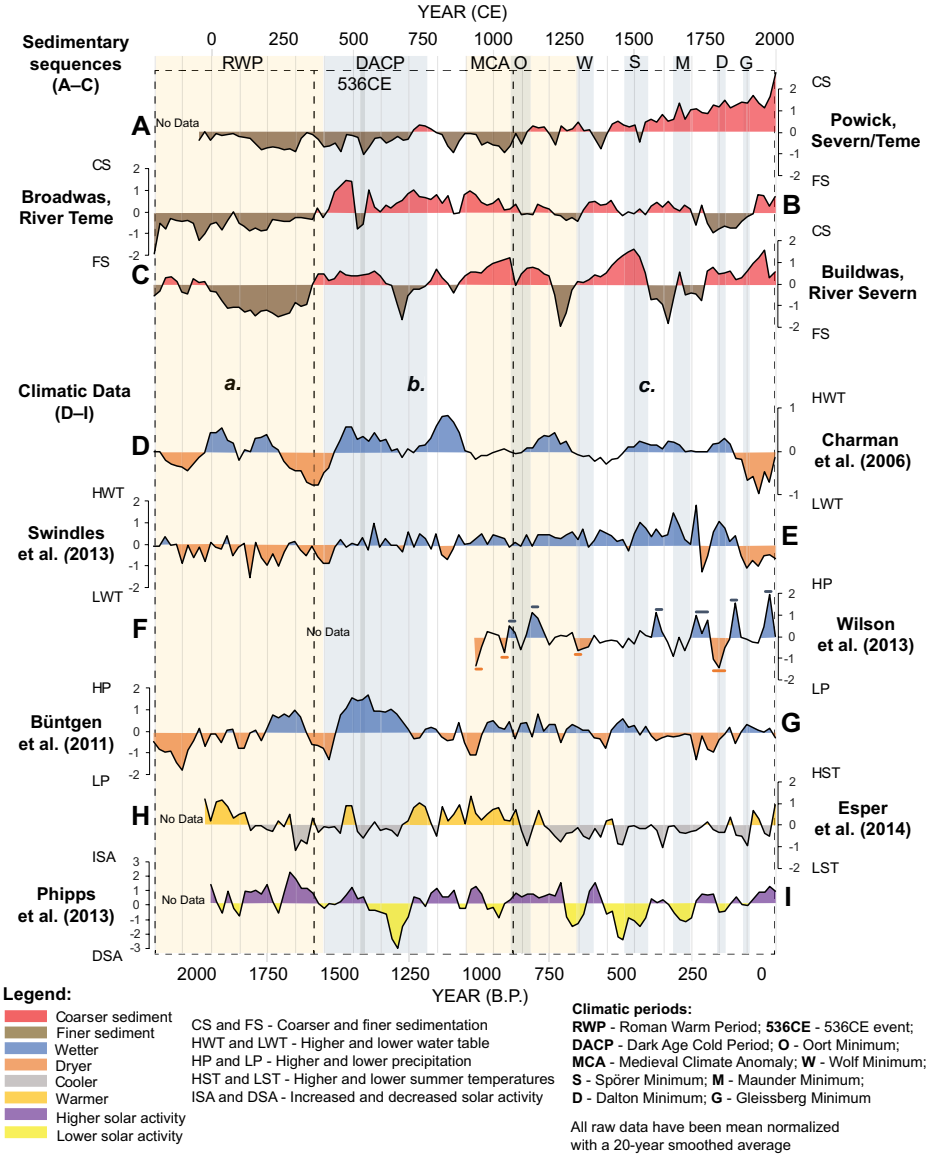

Figure 4. Sediment deposition models from the River Severn–River Teme confluence (United Kingdom) at Powick (A) with comparative models from sites upstream at Broadwas (Teme) (B) and Buildwas (Severn) (C), classified into three phases: (a) 20–400 CE; (b) 400–1100 CE; (c) 1100 CE–present. Also shown for comparison are upland peatland water table depth and proxy wetter-drier conditions in United Kingdom (D) and Ireland (E); precipitation in southern and central England (F) and central and southern Europe (G); summer temperatures in northern Europe (H); and solar activity variation (I).

land use and sediment erosion across the confluence landscape.

CONCLUSIONS

A combination of detailed topographic and sedimentological mapping, OSL dating, and stratigraphic modeling show that the river channels forming the Severn-Teme confluence zone have been almost completely fixed for the past 2000 yr. This has produced the continuous sedimentological record of levee and/or overbank flooding. High-resolution OSL dating of the sedimentary sequence has produced an alluvial flood record for the last two millennia. The sedimentary record shows distinct variation in depositionary conditions in the late Holocene, with phases of low- and high-magnitude events associated with changing land-use intensity in the surrounding local landscape in the medieval, post-medieval, and modern periods, and exacerbated by variable climatic drivers, especially during the Dark Age Cold Period, Medieval Climate Anomaly, and Little Ice Age.

ACKNOWLEDGMENTS

This work was undertaken as part of the Leverhulme Trust–funded "Flood and Flow" project (RPG-2016-004). We thank the landowners for access, the British Geological Survey for borehole records, and the UK Environment Agency for lidar data. The pOSL analysis was conducted using equipment owned by the University of Tromsø, Norway. We also thank the three anonymous reviewers for comments on the original manuscript.

REFERENCES CITED

Best, J.L., and Lane, S.N., 2004, Confluence, channel, and river junction, *in* Goudie, A.S., ed., Encyclopedia of Geomorphology: New York, Routledge, p. 180–183.

Blaauw, M., and Christen, J.A., 2011, Flexible palaeoclimate age-depth models using an autoregressive gamma process: Bayesian Analysis, v. 6, p. 457–474, https://doi.org/10.1214/11-BA618.

Black, A.R., and Law, F.M., 2004, Development and utilization of a national web-based chronology of hydrological events: Hydrological Sciences Journal, v. 49, p. 237–246, https://doi.org/10.1623/hysj.49.2.237.34835 .

British Geological Survey, 2017, Geoindex onshore borehole scans for the Severn-Teme confluence, SO85SW, SO85SE: Keyworth, Nottingham, UK, British Geological Survey, http://mapapps2.bgs.ac.uk/geoindex/home.html.

Broadberry, S., Campbell, B.M.S., Klein, A., Overton, M., and van Leeuwen, B., 2015, British Economic Growth, 1270–1870: Cambridge, UK, Cambridge University Press, 461 p., https://doi.org/10.1017/CBO9781107707603.

Bronk Ramsey, C., 2008, Deposition models for chronological records: Quaternary Science Reviews, v. 27, p. 42–60, https://doi.org/10.1016/j.quascirev.2007.01.019.

Bronk Ramsey, C., 2009, Bayesian analysis of radiocarbon dates: Radiocarbon, v. 51, p. 337–360, https://doi.org/10.1017/S0033822200033865.

Brown, A.G., 1985, Traditional and multivariate techniques in the interpretation of floodplain sediment grain size variations: Earth Surface Processes and Landforms, v. 10, p. 281–291, https://doi.org/10.1002/esp.3290100310.

Brown, A.G., 1987, Holocene floodplain sedimentation and channel response of the lower River Severn, U.K.: Zeitscrift für Geomorphologie, v. 31, p. 293–310.

Brown, A.G., 2009, Colluvial and alluvial response to land use change in Midland England: An integrated geoarchaeological approach: Geomorphology, v. 108, p. 92–106, https://doi.org/10.1016/j.geomorph.2007.12.021.

Brown, A., Toms, P., Carey, C., and Rhodes, E., 2013, Geomorphology of the Anthropocene: Time-transgressive discontinuities of human-induced alluviation: Anthropocene, v. 1, p. 3–13, https://doi.org/10.1016/j.ancene.2013.06.002.

Büntgen, U., et al., 2011, 2500 years of European climate variability and human susceptibility: Science, v. 331, p. 578–582, https://doi.org/10.1126/science.1197175.

Camporeale, C., Perona, P., Porporato, A., and Ridolfi, L., 2007, Hierarchy of models for meandering rivers and related morphodynamic processes: Reviews of Geophysics, v. 45, RG1001, https://doi.org/10.1029/2005RG000185.

Charman, D.J., Blundell, A., Chiverrell, R.C., Hendon, D., and Langdon, P.G., 2006, Compilation of non-annually resolved Holocene proxy climate records: Stacked Holocene peatland palaeo-water table reconstructions from northern Britain: Quaternary Science Reviews, v. 25, p. 336–350, https://doi.org/10.1016/j.quascirev.2005.05.005.

Croudace, I.W., Rindby, A., and Rothwell, R.G., 2006, ITRAX: Description and evaluation of a new multi-function X-ray core scanner, *in* Rothwell, R.G., ed., New Techniques in Sediment Core Analysis: Geological Society of London

Special Publication 267, p. 51–63, https://doi.org/10.1144/GSL.SP.2006.267.01.04.

Dixon, S.J., Sambrook Smith, G.H., Best, J.L., Nicholas, A.P., Bull, J.M., Vardy, M.E., Sarker, M.H., and Goodbred, S., 2018, The planform mobility of river channel confluences: Insights from remotely sensed imagery: Earth-Science Reviews, v. 176, p. 1–18, https://doi.org/10.1016/j.earscirev.2017.09.009.

Esper, J., Düthorn, E., Krusic, P.J., Timonen, M., and Büntgen, U., 2014, Northern European summer temperature variations over the Common Era from integrated tree-ring density records: Journal of Quaternary Science, v. 29, p. 487–494, https://doi.org/10.1002/jqs.2726.

Goldewijk, K. K. Beusen, A., and Janssen, P., 2010, Long-term dynamic modeling of global population and built-up area in a spatially explicit way: HYDE 3.1: The Holocene, v. 20, p. 565–573, https://doi.org/10.1177/0959683609356587.

Hey, G., 2004, Yarnton: Saxon and Medieval Settlement and Landscape—Results of Excavations 1990–96: Oxford Archaeology Thames Valley Landscapes Monograph 20, 465 p.

Lamb, H.H., 1972, Climate: Present, Past and Future: London, Routledge, 613 p.

Longfield, S.A., Faulkner, D., Kjeldsen, T.R., Macklin, M.G., Jones, A.F., Foulds, S.A., Brewer, P.A., and Griffiths, H.M., 2018, Incorporating sedimentological data in UK flood frequency estimation: Journal of Flood Risk Management, v. 12, e12449, https://doi.org/10.1111/jfr3.12449.

Macdonald, N., and Sangster, H., 2017, High-magnitude flooding across Britain since AD 1750: Hydrology and Earth System Sciences, v. 21, p. 1631–1650, https://doi.org/10.5194/hess-21-1631-2017.

Macklin, M.G., Jones, A.F., and Lewin, J., 2010, River response to rapid Holocene environmental change: Evidence and explanation in British catchments: Quaternary Science Reviews, v. 29, p. 1555–1576, https://doi.org/10.1016/j.quascirev.2009.06.010.

Macklin, M.G., Lewin, J., and Woodward, J.C., 2012, The fluvial record of climate change: Philosophical Transactions of the Royal Society A, v. 370, p. 2143–2172, https://doi.org/10.1098/rsta.2011.0608.

Marsh, T., Kirby, C., Muchan, K., Barker, L., Henderson, E., and Hannaford, J., 2016, The winter floods of 2015/2016 in the UK—A review: Wallingford, UK, Centre for Ecology & Hydrology, 37 p.

Muñoz-Salinas, E., Bishop, P., Sanderson, D.C.W., and Zamorano, J.-J., 2010, Interpreting luminescence data from a portable OSL reader: Three case studies in fluvial settings: Earth Surface Processes and Landforms, v. 36, p. 651–660, https://doi.org/10.1002/esp.2084.

Pears, B., Brown, A.G., Carroll, J., Toms, P., Wood, J., and Jones, R., 2020, Early medieval place-names and riverine flood histories: A new approach and new chronostratigraphic records for three English rivers: European Journal of Archaeology, p. 1–25, https://doi.org/10.1017/eaa.2019.72.

Phipps, S.J., McGregor, H.V., Gergis, J., Gallant, A.J.E., Neukom, R., Stevenson, S., Ackerley, D., Brown, J.R., Fischer, M.J., and van Ommen, T.D., 2013, Paleoclimate data-model comparison and the role of climate forcings over the past 1500 years: Journal of Climate, v. 26, p. 6915–6936, https://doi.org/10.1175/JCLI-D-12-00108.1.

Rippon, S., Smart, C., and Pears, B., 2015, The Fields of Britannia: Oxford, UK, Oxford University Press, 416 p.

Robinson, M.A., and Lambrick, G.H., 1984, Holocene alluviation and hydrology in the upper Thames basin: Nature, v. 308, p. 809–814, https://doi.org/10.1038/308809a0.

Rumsby, B.T., and Macklin, M.G., 1996, River response to the last neoglacial (the 'Little Ice Age') in northern, western and central Europe, *in* Branson, J., et al., eds., Global Continental Changes: The Context of Palaeohydrology: Geological Society of London Special Publication 115, p. 217–233, https://doi.org/10.1144/GSL.SP.1996.115.01.17.

Sanderson, D.C.W., and Murphy, S., 2010, Using simple portable OSL measurements and laboratory characterisation to help understand complex and heterogeneous sediment sequences for luminescence dating: Quaternary Geochronology, v. 5, p. 299–305, https://doi.org/10.1016/j.quageo.2009.02.001.

Shotton, F.W., 1978, Archaeological inferences from the study of alluvium in the lower Severn-Avon valleys, *in* Limbrey, S., and Evans, J.G., eds, The Effect of Man on the Landscape: The Lowland Zone: Council for British Archaeology Research Report 21, p. 27–32.

Swindles, G.T., et al., 2013, Centennial-scale climate change in Ireland during the Holocene: Earth-Science Reviews, v. 126, p. 300–320, https://doi.org/10.1016/j.earscirev.2013.08.012.

UK Environment Agency, 2016, Raw lidar data, 1 m DTM (2016) for SO85SW, SO85SE: Department for Environment, Food and Rural Affairs, HMSO, https://environment.data.gov.uk/DefraDataDownload/?Mode=survey.

UK Ordnance Survey, 1886,UK Ordnance Survey County Series 1st Edition, 1886, [TIFF geospatial data], scale 1:2500, Tiles: worc-so8149-1,worc-so8150-1,worc-so8151-1,worc-so8152-1,worc-so8249-1,worc-so8250-1,worc-so8251-1,worc-so8252-1,worc-so8349-1,worc-so8350-1,worc-so8351-1,worc-so8352-1,worc-so8449-1,worc-so8450-1,worc-so8451-1,worc-so8452-1. Updated 30 November 2010 (downloaded from EDINA Historic Digimap Service, http://digimap.edina.ac.uk, on 2017-07-20 17:40:25.966).

UK Ordnance Survey, 2016, Raw lidar data, 50 m DTM for grid squares SO85SW, SO85SE, 1:50,000, https://digimap.edina.ac.uk/roam/download/os (extracted and downloaded from Edina digimap [2017-07-20]).

Wanner, H., et al., 2008, Mid- to Late Holocene climate change: An overview: Quaternary Science Reviews, v. 27, p. 1791–1828, https://doi.org/10.1016/j.quascirev.2008.06.013.

Williamson, T., 2013, Environment, Society and Landscape in Early Medieval England: Time and Topography: Woodbridge, UK, The Boydell Press, Anglo-Saxon Studies, v. 19, 280 p.

Wilson, R., Miles, D.., Loader, N.J., Melvin, T., Cunningham, L., Cooper, R., and Briffa, K., 2013, A millennial long March–July precipitation reconstruction for southern-central England: Climate Dynamics, v. 40, p. 997–1017, https://doi.org/10.1007/s00382-012-1318-z.

Printed in USA